AD-A090 945 NAVAL RESEARCH LAB WASHINGTON DC F/G 20/11
PHOTOELASTIC STRESS AND FRACTURE ANALYSIS OF TWO NEUTRON TUBE D--ETC(U)
OCT 80 V J PARKS, R J SANFORD
UNCLASSIFIED NRL-MR-4363 NL

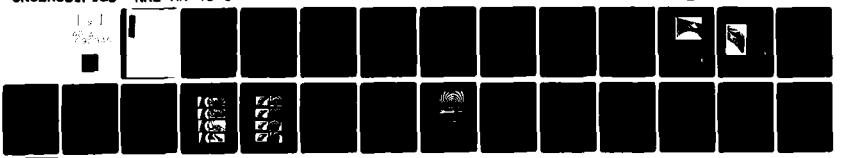

END
DATE FILMED
12-80
DTIC

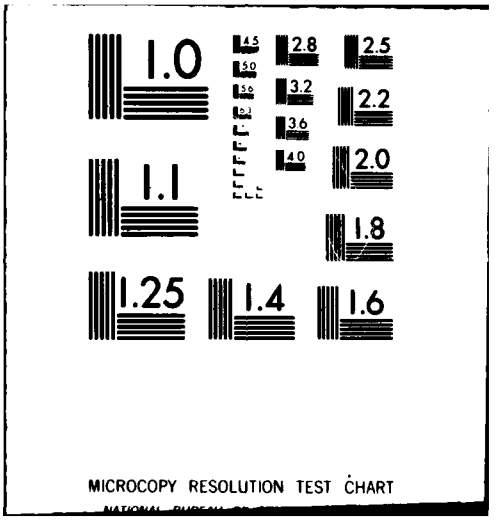
1.0
1.1
1.25
1.4
1.6
1.8
2.0
2.2
2.5
2.8
3.2
3.6
4.0
4.5
5.0
5.6
6.3
MICROCOPY RESOLUTION TEST CHART

SECURITY CLASSIFICATION OF THIS PAGE (When Data Entered)

REPORT DOCUMENTATION PAGE

READ INSTRUCTIONS BEFORE COMPLETING FORM

1. REPORT NUMBER: NRL Memorandum Report 4363
2. GOVT ACCESSION NO.: AD-A090 945
3. RECIPIENT'S CATALOG NUMBER:

4. TITLE (and Subtitle): PHOTOELASTIC STRESS AND FRACTURE ANALYSIS OF TWO NEUTRON TUBE DESIGNS
5. TYPE OF REPORT & PERIOD COVERED: Final Report
6. PERFORMING ORG. REPORT NUMBER:

7. AUTHOR(s): V. J. Parks and R. J. Sanford
8. CONTRACT OR GRANT NUMBER(s): (DOE Appropriation 89X0210) 13-8305

9. PERFORMING ORGANIZATION NAME AND ADDRESS: Naval Research Laboratory, Washington, D.C. 20375
10. PROGRAM ELEMENT, PROJECT, TASK AREA & WORK UNIT NUMBERS: DOE 81934, 84-0285-0-0

11. CONTROLLING OFFICE NAME AND ADDRESS: Sandia Laboratories, Albuquerque, New Mexico 87185
12. REPORT DATE: 15 October 1980
13. NUMBER OF PAGES: 25

14. MONITORING AGENCY NAME & ADDRESS (if different from Controlling Office): NRL-MR-4363
15. SECURITY CLASS. (of this report): Unclassified
15a. DECLASSIFICATION/DOWNGRADING SCHEDULE:

16. DISTRIBUTION STATEMENT (of this Report): Approved for public release; distribution unlimited.

17. DISTRIBUTION STATEMENT (of the abstract entered in Block 20, if different from Report):

18. SUPPLEMENTARY NOTES:

19. KEY WORDS (Continue on reverse side if necessary and identify by block number)

Stress Analysis	Computer Graphics
Fracture Mechanics	Finite Elements
Photoelasticity	Neutron Tube

20. ABSTRACT (Continue on reverse side if necessary and identify by block number)

Photoelastic stress analysis and fracture stress analysis were carried out on two-dimensional models of the cross-sections of the M5N and M19N designs of a neutron tube under axial load. Of special interest was the metal-ceramic interface, where failure had been experienced. Both types of analysis showed the M5N to be superior to the M19N for the given loading in the area of failure. Tangential stresses along the free surfaces, and mixed-mode stress intensity factors for various crack lengths along the interface are reported.

DD FORM 1 JAN 73 1473 EDITION OF 1 NOV 65 IS OBSOLETE
S/N 0102-014-6601

CONTENTS

PHOTOELASTIC STRESS AND FRACTURE ANALYSIS OF TWO NEUTRON TUBE DESIGNS

INTRODUCTION

A neutron tube is a small axisymmetric component, composed of inner and outer metal sleeves separated by a glass ceramic insulator. The Sandia Corporation is conducting a series of strength tests on various neutron tube designs. Test results indicate that premature failures are occuring at or near the bond between the inner sleeve and the insulator. Examination of the failed specimens indicated that catastrophic failure is proceeded by a short period of slow crack growth at the interface. In order to better understand the mechanism of failure, Sandia has conducted an extensive series of analyses on various tube designs.

This report describes stress and failure analyses on two candidate tube designs by the Naval Research Laboratory. NRL considered one loading, a uniform, axial, axisymmetric load acting on the protruding end of the inner sleeve and reacted at the opposite end of the outer sleeve. This loading simulates the conditions of one of the strength tests on the prototype parts conducted by Sandia. The load and geometries are shown in Fig. 1.

CONSIDERATION OF THE METHOD OF ANALYSIS

The stress field in the neutron tube is axisymmetric since both geometry and load are axisymmetric. The materials of the neutron tube are the ceramic of the insulator and the metal of the inner and outer sleeves which has a Young's modulus approximately four times that of the ceramic. The need to obtain stresses and stress intensity factors near and on the interface of the two dissimilar materials is the most difficult feature of the problem.

Manuscript submitted August 21, 1980.

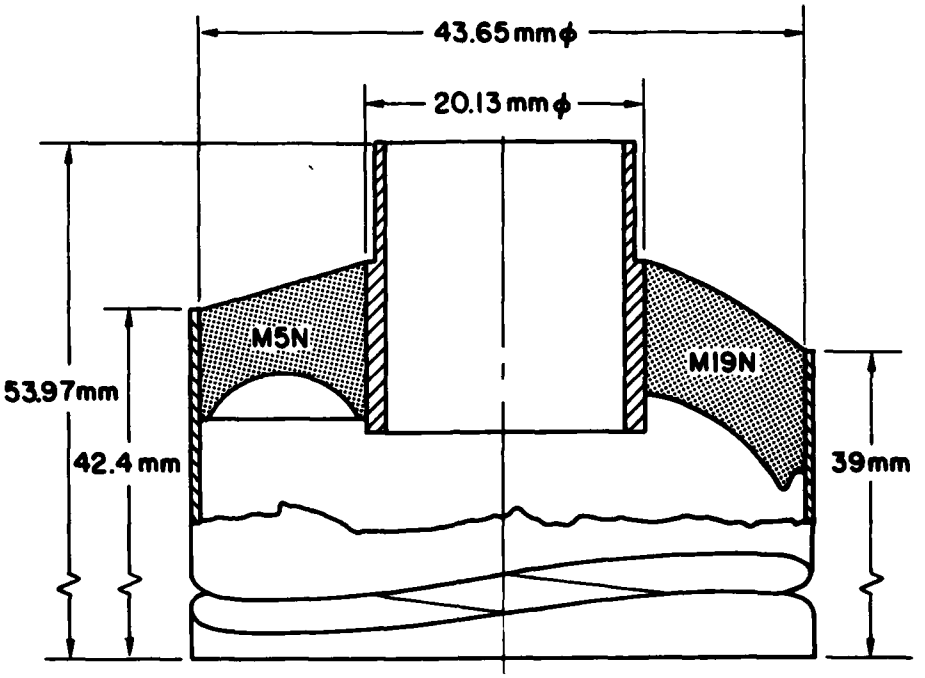

SCHEMATIC SHOWING CROSS SECTIONS OF BOTH DESIGNS

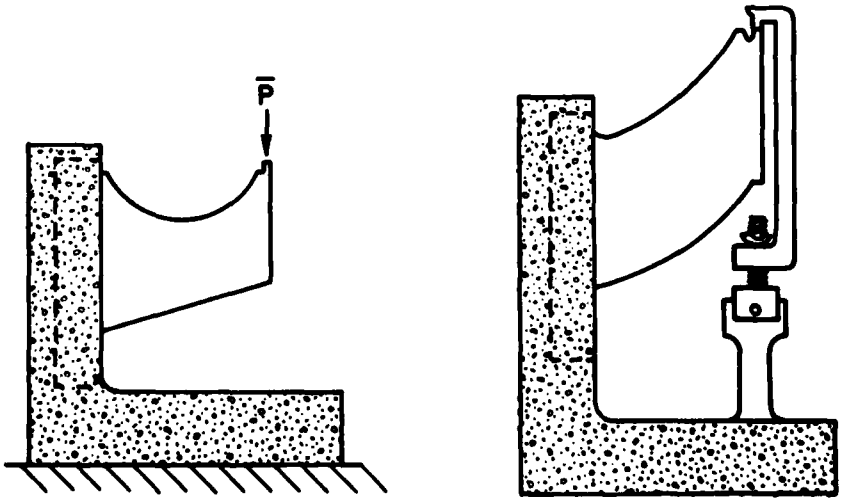

2D MODEL OF M5N WITH MACHINE LOAD

2D MODEL OF M19N WITH AUTOCALIBRATION SETUP

Fig. 1 — Geometry and loading of M5N and M19N neutron tube designs and models

A number of methods of analysis were considered. Classical theoretical methods of stress analysis would find difficulty in representing the boundary conditions. Finite element methods typically give poor results on and near the interface. There is no practical experimental way to measure the actual stresses on the interface of the prototype. Three-dimensional bi-material photoelastic modeling would be costly and time consuming. Thus, it was decided to conduct an approximate analysis using two-dimensional photoelastic models of the cross section.

The rationale for approximating the axisymmetric problem with a plane-stress, two-dimensional model can best be described in two steps; (1) the rationale for representing the cross section of the axisymmetric geometry with the cross section of the corresponding plane-strain geometry, and (2) representing the plane strain cross section with a similar plane stress model.

First Step

The solution of the plane-strain case approaches the axisymmetric solution as the ratio of the inner to outer radius approaches unity. Clearly in the neutron tube the radius ratio is not near unity. The approximation is justified for the neutron tube analysis by two observations. The first observation, based on the principle of equilibrium, is that most of the stress variation between the plane strain case and an axisymmetric case, with a radius ratio far less than unity, is due to the gradual increase in area of a representative angular (pie-shaped) segment of the axisymmetric geometry as compared to a uniform thickness slice of the plane strain geometry. So that, if the same force is applied at the inner radius of the axisymmetric geometry as at the corresponding position on the plane strain geometry, the in-plane stresses at the outer radius of the axisymmetric geometry will be less than at the corresponding area of the plane strain geometry by approximately the ratio of the inner to outer radius. A corresponding reduction will occur at all intermediate points. Thus in-plane stress could be adjusted to better approximate the axisymmetric case by a simple geometric correction factor. The second observation is that the variation between the axisymmetric and plane strain stress fields cited above, and any other secondary differences, will be the same for the various design changes, since the radius ratio is

fixed in all cases, and the radial location of failure is the same for all designs. Thus for purposes of comparison of designs the stress proportion will be the same.

Second Step

The plane-strain-plane-stress correspondence is a well accepted principle in elastic analysis and states that, given certain conditions, the stress fields in plane-strain and plane-stress are exactly the same. One of the conditions is that the problem be of a "first-boundary value" type. The metal-to-ceramic interfaces of the cross-section violate this condition. Thus the plane stress solution will not be exactly the same as the plane strain solution. This is especially true in the vicinity of the bonded interface. Here again, as in the first step, some engineering judgment must be used to decide if the modeling gives a valid approximation.

The stress analyses have been confined to the free boundaries and so are considered good approximations of the plane strain case.

The fracture mechanics analyses on the other hand seek to determine the K-factor on the bonded interface. Fracture mechanics methods have long dealt with plane-stress-plane-strain correspondence, since any crack because of it very small tip radius must be considered to have a plane strain region about the tip, whilst away from the tip many problems have a plane stress character. Between the crack tip and the plane stress region there is a transition region from plane strain to plane stress. (This transition region may also contain nonlinear or plastic stresses and strains.) To avoid the transition zone, (and also non-linearity and plasticity), stress measurements are typically made at least one-third of the model thickness from the crack tip. This procedure was followed in all the analyses reported here. Thus all measurements were made far enough from the bonded interface to obtain valid analysis.

The rigidity of the inner metal sleeve was simulated with a pair of metal clamps on either side of the 2-D photoelastic model. A similar arrangement could have been used to simulate the outer sleeve. This was not done because it was felt that this variation would be influential only near the outer sleeve, and would have only slight effect over most of the stress field, and not be a factor on the stresses at the

inner sleeve. This assumption was confirmed from 2-D finite element analysis of the various conditions.

EXPERIMENTS

Two-dimensional photoelastic models were made of the cross sections of two neutron tube designs, M5N and M19N. The model of the M5N cross section was 16 times actual size, and the M19N model was 10 times actual. The portion of each model representing the inner sleeve was fixed between a pair of rigid plates. Axial load was applied to the portion of the model representing the outer sleeve.

Light and dark field isochromatic patterns were photographed at various load levels on both models. After the isochromatics for the stress analysis were obtained, the same models were used for fracture analysis. The models were removed from the rigid clamps and a cut was made along the line of the inner-sleeve- insulator interface to simulate a crack where fractures had been observed. This cut was made with a thin saw in some models and an angled milling cutter in others. The models were replaced in the rigid clamp and reloaded. Light and dark field isochromatics of the loaded model with the simulated crack were photographed as before, and in addition close-up photographs of the crack tip region were taken. This process was repeated a number of times for each model, lengthening the simulated crack at each step.

ANALYSIS AND RESULTS

Stresses are obtained from the isochromatic patterns from the stress-optic law

$$\sigma_1 - \sigma_2 = 2\,\tau_{max} = nf/t \qquad (1)$$

where σ_1 and σ_2 are principal stresses at a point, τ_{max} is the maximum shear stress at the point, n is the fringe order at the point, f is the stress-optic coefficient (a constant) and t is the model thickness.

On free boundaries of the model (in particular the free surfaces of the insulator) one of the principal stresses is zero and this equation reduces to

$$\sigma = nf/t \tag{2}$$

In the dark field isochromatic pattern, the fringe orders are integers (n = 0, 1, 2, 3 ...) and are easily identified. The light field fringes are the half order values (n = 0.5, 1.5, 2.5 ...). Intermediate fringe values of n can be obtained with simple photoelastic techniques to an accuracy of about 0.01 fringe. Dark field photoelastic patterns from the M5N and M19N models are shown in Figs. 2 and 3 respectively. Also shown in Figs. 2 and 3 are corresponding numerical solutions, obtained with TOTAL, an NRL developed, graphics-oriented, finite element library [1].

To solve for the stress it is customary to determine the value of the coefficient f using a simple calibration model with a known stress field, of the same material and thickness as the model. The calibration model is customarily loaded and f determined. In some of the models this approach was modified by putting the calibration model, a tensile strip, in the load train with the neutron tube model so each was subjected to the same load. The load was applied as shown in Figure 1.

The same equation applied to the free boundary also applied to the tensile strip, since the transverse stress in the strip is zero

$$\sigma_c = n_c f/t \tag{3}$$

where the subscript c is used to indicate calibration.

The load in both the tensile strip and in the model is

$$P = (\sigma_c)(A_c) = n_c f(w_c\, t_c)/t_c \tag{4}$$

where A_c is the cross-sectional area of the tensile strip and w_c is the width of the tensile strip.

The expression for load reduces to

$$P = n_c\, f\, w_c \tag{5}$$

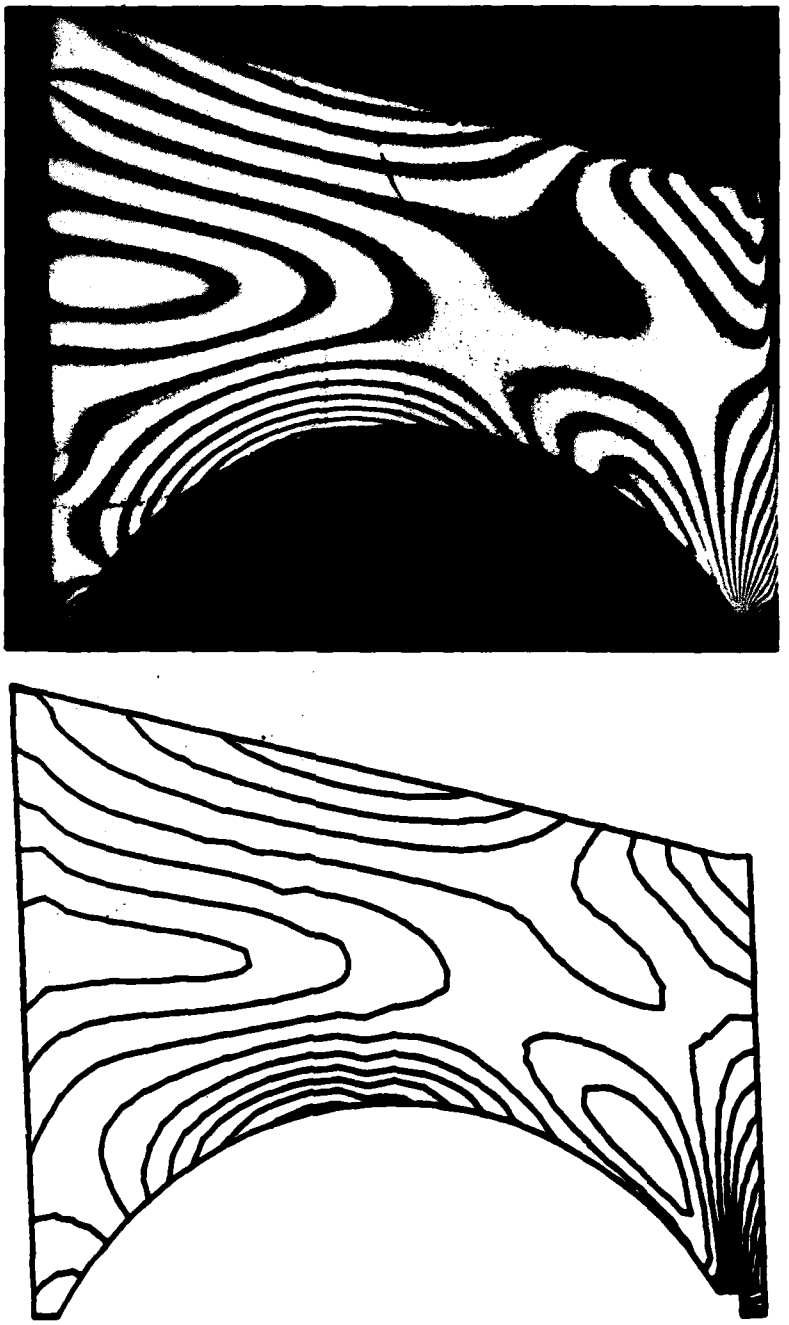

Fig. 2 — Dark field isochromatic pattern from model of M5N cross-section. Finite element solution is shown for comparison.

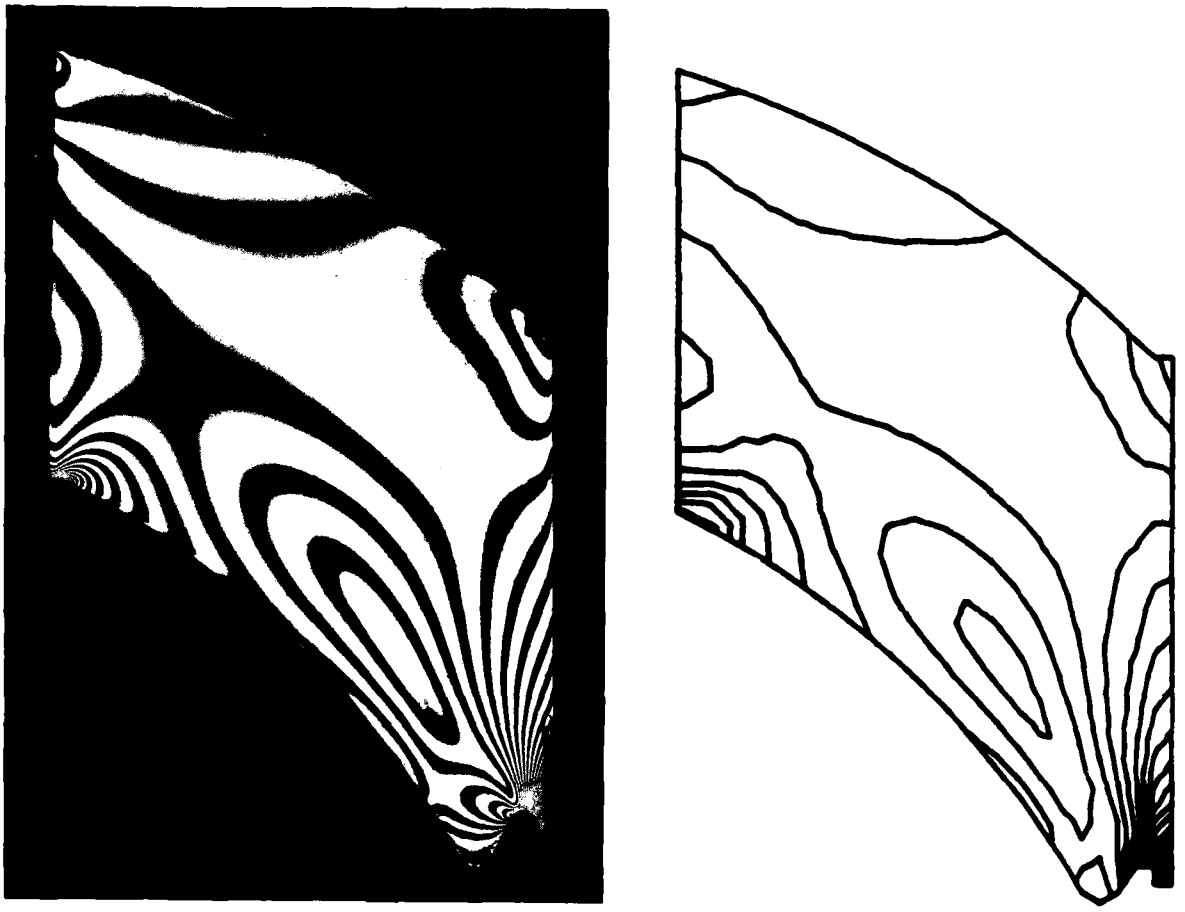

Fig. 3 — Dark field isochromatic pattern from model of M19N cross-section. Finite element solution is shown from comparison.

Combining Eq. (5) with Eq. (2) eliminates f

$$\sigma = \frac{n}{t} \frac{P}{n_c w_c} \tag{6}$$

The ratio, P/t, is the load per unit thickness, letting $\bar{P} = P/t$, Eq. (6), for the boundary stress can be written

$$\frac{\sigma}{\bar{P}} = \frac{n}{n_c} \frac{1}{w_c} \tag{7}$$

The terms of the equation have the dimension of the reciprocal of length. Multiplying the equation by a representative length on the model gives a non-dimensional equation and a non-dimensional (normalized) expression for stress. The length of the inner-sleeve-insulator interface is designated L and

$$\frac{\sigma L}{\bar{P}} = \frac{n}{n_c} \frac{L}{w_c} \tag{8}$$

This approach, referred to as auto-calibration, permits determination of the normalized stress without knowledge or measurement of model load, stress-optic coefficient, model thickness and calibration thickness. However, these values were determined as secondary checks.

The normalized stress is obtained from four measurements; n, n_c, L and w_c. w_c is the same for all tests, 2.000 inches. L is 6.400 inches on the M5N model and 4.000 inches on the M19N model. n_c varied with load and values from 0.95 to 2.75 were used. The n value, of course, varied with model, load and position. Values of up to $n = 31.0$ were recorded.

Once the $\sigma L/\bar{P}$ ratio has been established for any point on a model, it is valid at that point for any load, and any size model, including the actual neutron tubes it represents. The L for both neutron tube designs is 10.16 mm (0.40 inches). For a given load per unit length $\bar{P}$, the stress at a given point is obtained by multiplying the $\sigma L/\bar{P}$ ratio by $\bar{P}/L$.

The normalized stresses on the free boundaries of the M5N and M19N insulator are given in Figs. 4 and 5 respectively.

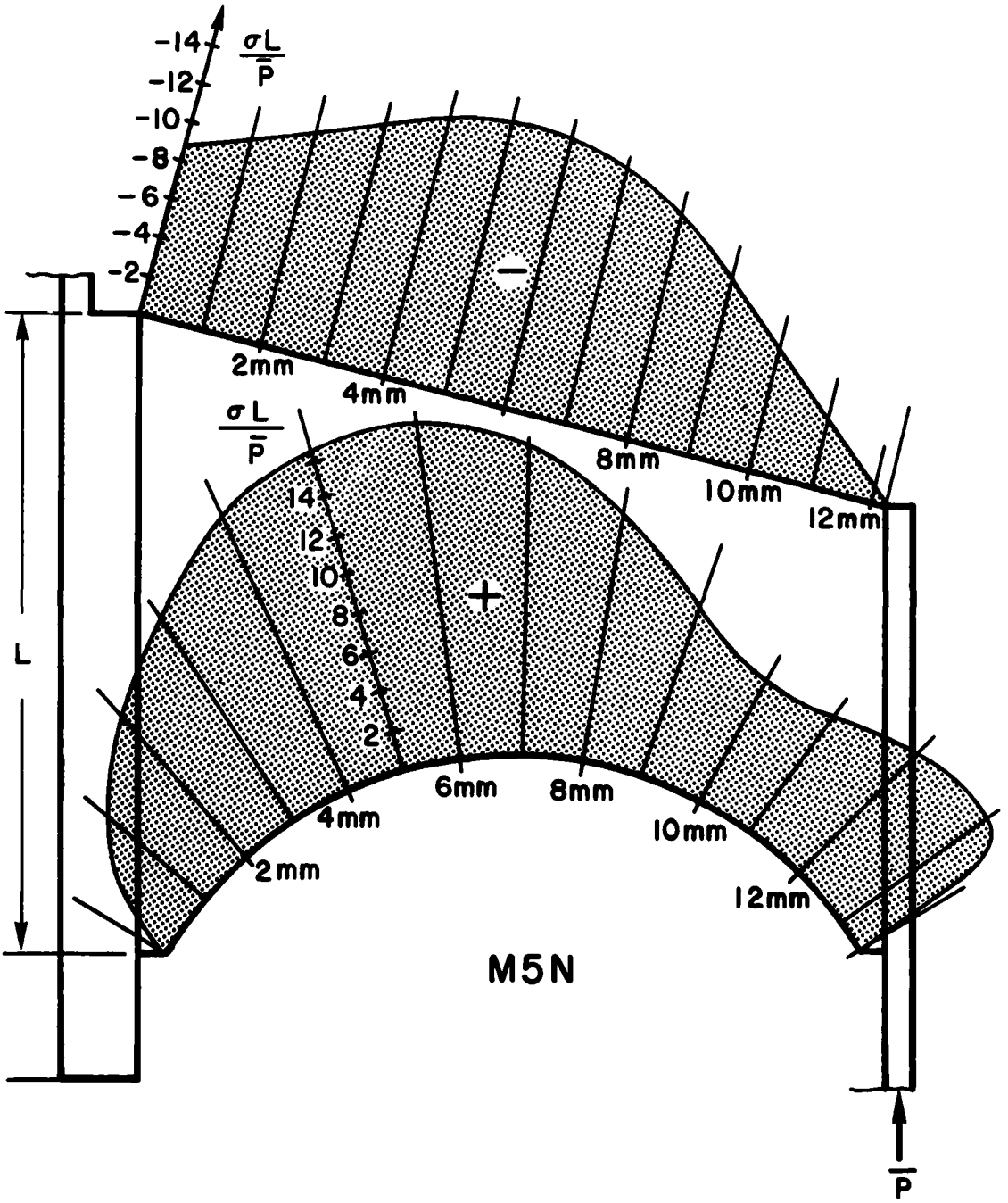

Fig. 4 — Normalized tangential stresses on free boundaries of M5N neutron tube

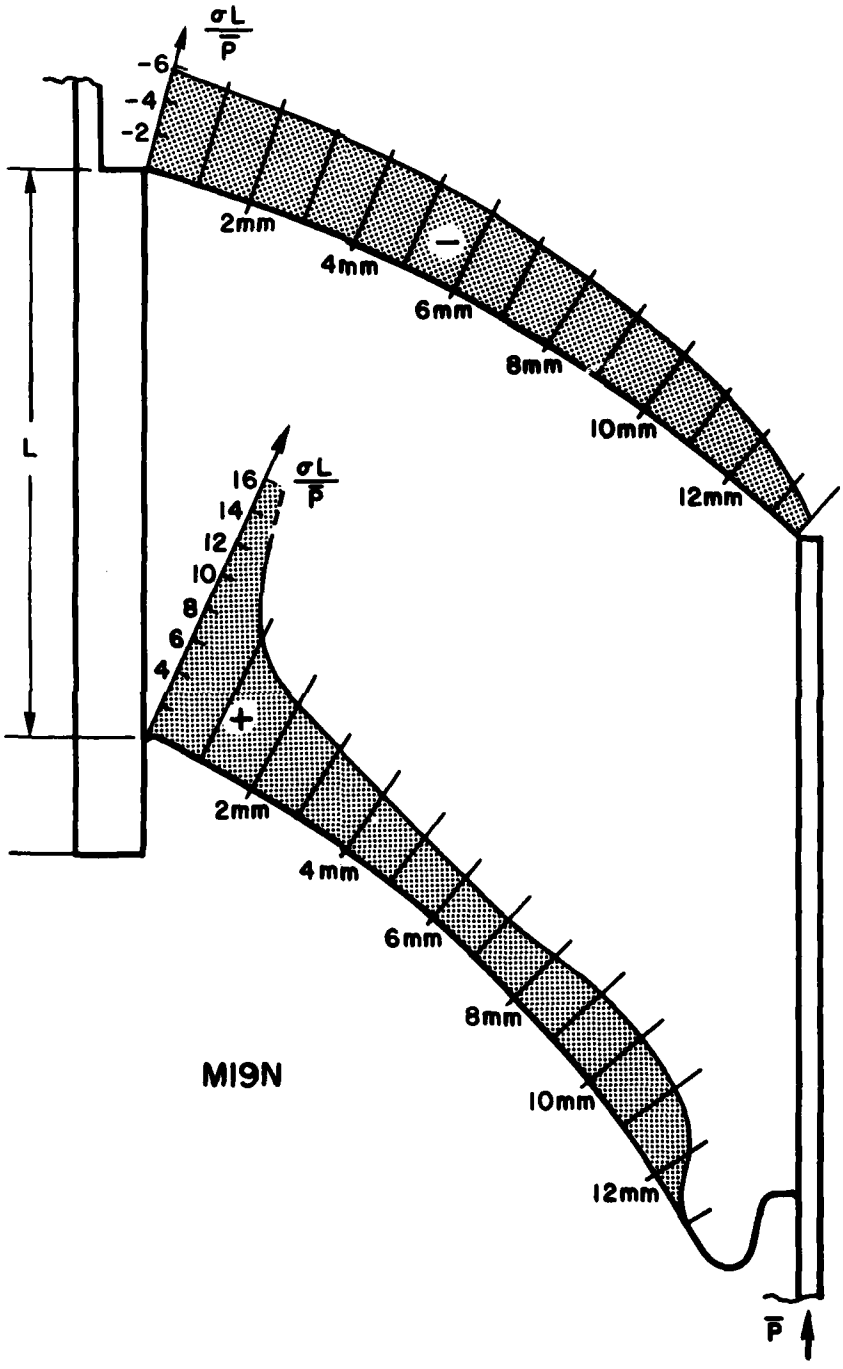

Fig. 5 — Normalized tangential stresses of free boundaries of M19N neutron tube

The stress intensity factors (SIF) for various crack lengths were obtained from the same models used to obtain stresses on the free boundaries, and some of the analysis was similar. Overall views and close-ups of the crack tip for the M5N and M19N models at various steps of cracking are shown in Figs. 6 and 7 respectively. For the fracture analysis a more general form of Eq. (8) gives the principal stress difference

$$\frac{(\sigma_1 - \sigma_2)L}{\bar{P}} = \frac{n}{n_c}\frac{L}{w_c}. \tag{9}$$

The principal stress difference is in turn related to the opening mode SIF, K_I, the shear mode SIF, K_{II}, and the far field stress, σ_{ox}, by a form of the Irwin-Sneddon equations. The Irwin-Sneddon equations, which approximate the stress field in the local neighborhood of a crack tip ($r/l \ll 1$) are usually written in terms of the Cartesian stresses

$$\sigma_x = \frac{1}{\sqrt{(2\pi r)}}\left[K_I \cos\frac{\theta}{2}\left\{1 - \sin\frac{\theta}{2}\sin\frac{3\theta}{2}\right\} - K_{II}\sin\frac{\theta}{2}\left\{2 + \cos\frac{\theta}{2}\cos\frac{3\theta}{2}\right\}\right] - \sigma_{ox}$$

$$\sigma_y = \frac{1}{\sqrt{(2\pi r)}}\left[K_I \cos\frac{\theta}{2}\left\{1 + \sin\frac{\theta}{2}\sin\frac{3\theta}{2}\right\} + K_{II}\sin\frac{\theta}{2}\cos\frac{\theta}{2}\cos\frac{3\theta}{2}\right]$$

$$\tau_{xy} = \frac{1}{\sqrt{2\pi r}}\left[K_I \sin\frac{\theta}{2}\cos\frac{\theta}{2}\cos\frac{3\theta}{2} + K_{II}\cos\frac{\theta}{2}\left\{1 - \sin\frac{\theta}{2}\sin\frac{3\theta}{2}\right\}\right] \tag{10}$$

where x and y are Cartesian coordinates, and r and θ are polar coordinates, with the origin in both coordinate systems defined at the crack tip. The crack has length l and is located on the negative x-axis ($\theta = 180°$).

The principal stress difference is related to the Cartesian stresses by:

$$(\sigma_1 - \sigma_2)^2 = (\sigma_x - \sigma_y)^2 + (2\,\tau_{xy})^2. \tag{11}$$

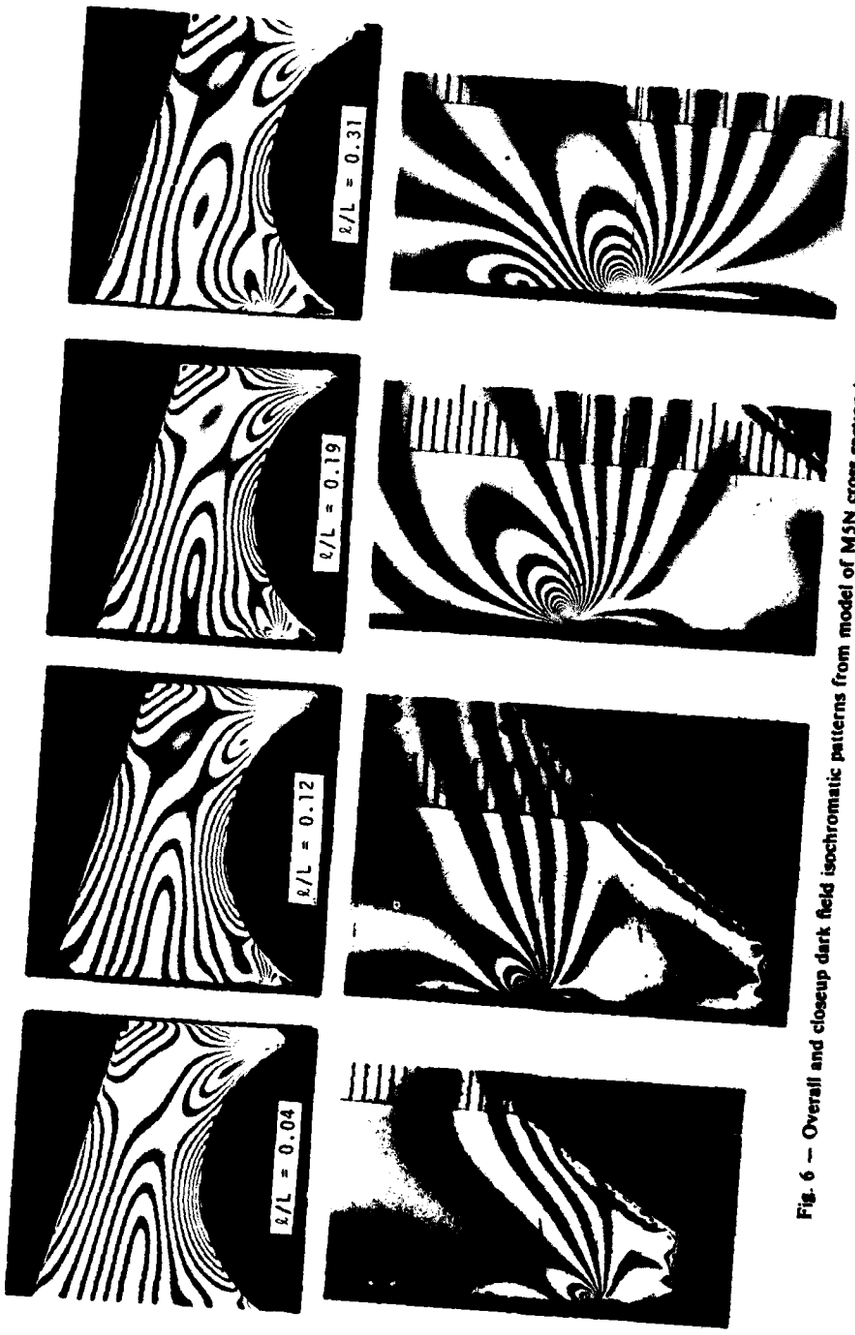

Fig. 6 — Overall and closeup dark field isochromatic patterns from model of M5N cross section for various crack lengths

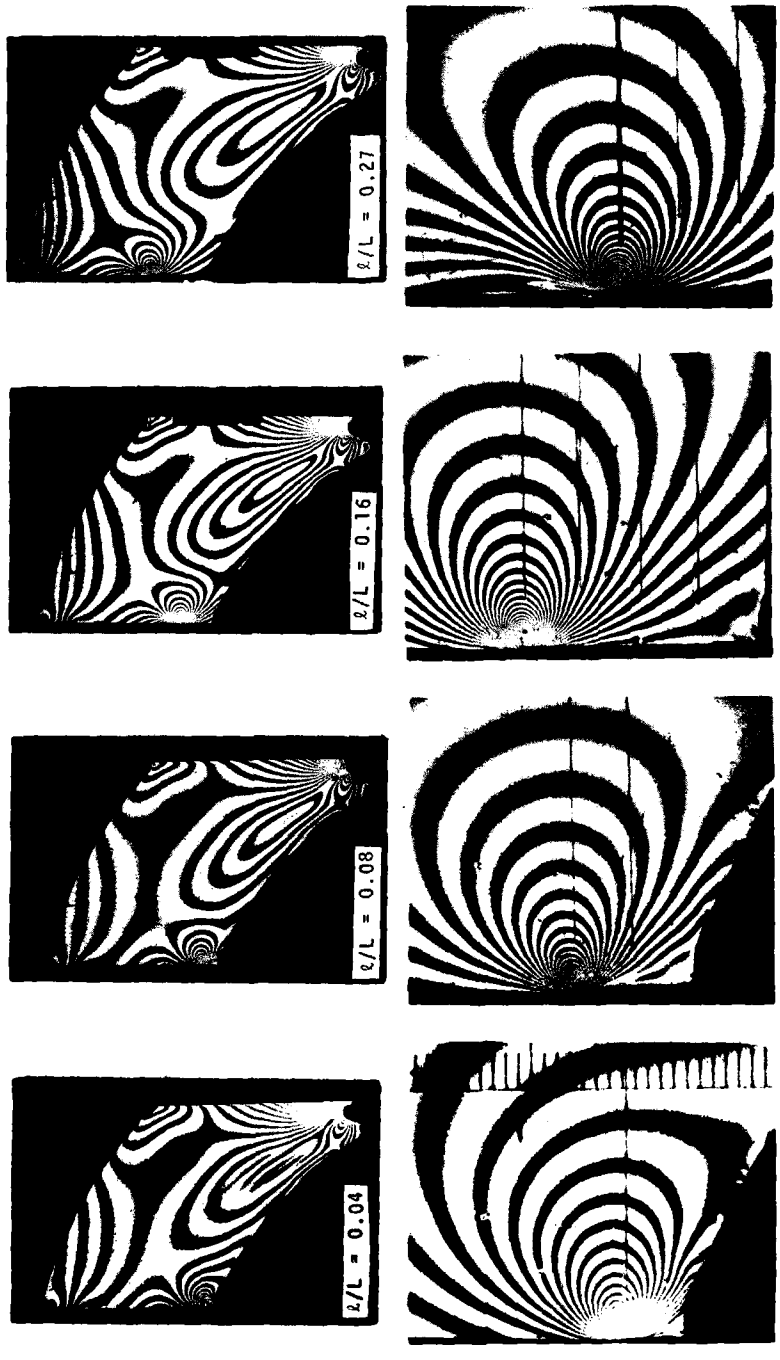

Fig. 7 — Overall and closeup dark field isochromatic patterns from model of M19N cross section for various crack lengths

Substituting Eq. (10) in Eq. (11) and normalizing as before gives

$$\left[\frac{(\sigma_1-\sigma_2)L}{\bar{P}}\right]^2 = \frac{1}{2\pi^2(r/L)}\left[\left(\frac{K_I\sqrt{\pi L}}{\bar{P}}\sin\theta + 2\,\frac{K_{II}\sqrt{\pi L}}{\bar{P}}\cos\theta\right)^2 + \left(K_{II}\,\frac{\sqrt{\pi L}}{\bar{P}}\sin\theta\right)^2\right] \tag{12}$$

$$+ 2\,\frac{\sigma_{ox}L}{\bar{P}}\,\frac{\sin(\theta/2)}{\pi\sqrt{2r/L}}\left[\frac{K_I\sqrt{\pi L}}{\bar{P}}\sin\theta(1+2\cos\theta)\right.$$

$$\left. + \frac{K_{II}\sqrt{\pi L}}{\bar{P}}\,(1+2\cos^2\theta+\cos\theta)\right] + \left[\frac{\sigma_{ox}L}{\bar{P}}\right]^2$$

For a given point, (r, θ), with a known value of $\frac{(\sigma_1-\sigma_2)L}{\bar{P}}$ determined from Eq. (1), this is an equation in three unknowns: $K_I\sqrt{\pi L}/\bar{P}$, $K_{II}\sqrt{\pi L}/\bar{P}$ and $\sigma_{ox}L/\bar{P}$. Using data from just three points on the model, the three corresponding equations could be solved for the unknowns. Using just three points could lead to significant error, by selection of insensitive points and the usual measurement errors [2]. To avoid these difficulties 20 diverse points were selected from each light and dark field photograph in the vicinity of the crack tip.

The 20 points generated 20 equations. An overdeterministic method using least squares [2,3] was used to obtain the three variables for eight different crack lengths on each of the two designs M5N and M19N. Several models of the M5N were tested with differing procedures. The variables were computed with all 20 points in each field, but were also computed with a number of subsets of the 20 points, and with the origin shifted, to probe for any significant errors in the analysis.

All the SIF values obtained were checked by putting each set of K_I, K_{II} and σ_{ox} values into Eqs. (9-11) and calculating the fringe order at each measurement point. The standard deviation of the difference between the measured fringes and the calculated fringes was used to estimate error in the analysis. For the M19N data only 3 out of 16 sets had a standard deviation greater than half of a fringe order. All the saw-cut M5N models showed a standard deviation of less than half a fringe. On the mill-cut M5N model, 5 out of 8 had a standard deviation of less than half of a fringe order.

This same approach was used to generate graphic displays of fringe patterns for a number of sets of K_I, K_{II} and σ_{ox}. One such set is shown in Fig. 8 with the corresponding photoelastic pattern. Visual comparisons of the fringe patterns confirmed in all cases that the determined SIF values did indeed represent the analyzed crack.

The opening mode SIF and the shear mode SIF, as well as the resultant stress intensity factor, $K = \sqrt{K_I^2 + K_{II}^2}$, are plotted in dimensionless form in Figs. 9 and 10 for the M5N model and in Figs. 11 and 12 for the M19N model.

DISCUSSION OF THE RESULTS

Stress Analysis

The photoelastic patterns in Figs. 2 and 3 and the normalized stress plots in Figs. 4 and 5 all indicate that overall the stresses are greater in the M5N than in the M19N cross section. However in the critical area, at the end of the inner-sleeve- insulator interface where failure begins, the stress in the M5N cross section is reduced appreciably. This is largely due to the insulator lip in the critical area, characterized by the large obtuse angle between the free surface of the inner sleeve and the free surface of the insulator. The fairing of this insulator lip attenuates the stress in the critical area.

The M19N geometry creates just the reverse effect. The overall "arch" shape is more efficient in transmitting the forces between the inner and outer sleeve and thus overall the stresses are less than those of the M5N cross section. However, the "arch" creates an acute angle at the end of the inner-sleeve-insulator interface that multiplies rather than attenuates the overall stress, and so creates higher stresses in the critical area than found in the M5N cross section.

The stress analysis indicates the M19N cross section is more likely to fail at the interface than the M5N cross section.

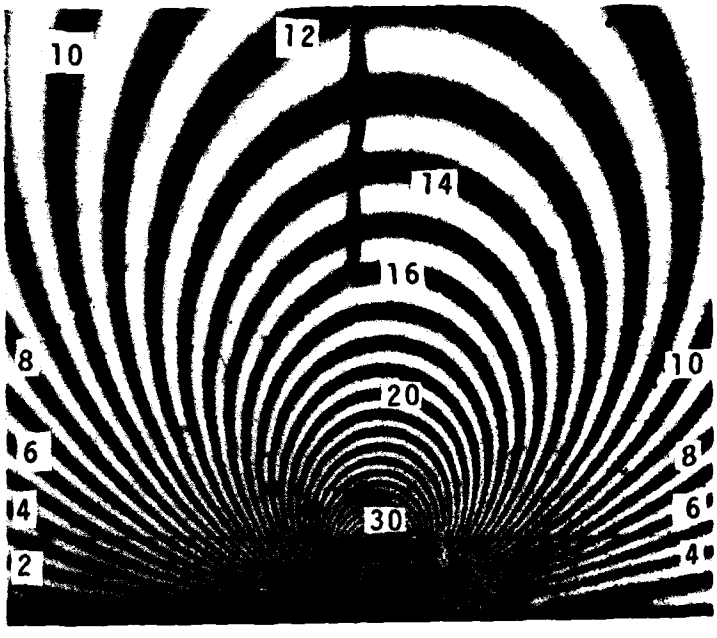

0.1 mm PROTOTYPE

1.0 mm MODEL

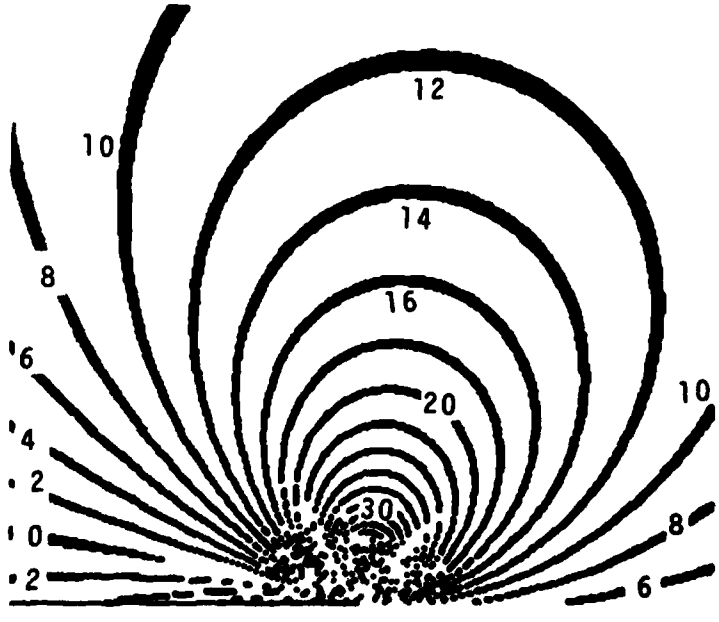

Fig. 8 — Dark field isochromatic pattern and pattern regenerated from stress intensity factors from the M19N mode with a length of $l/L = 0.16$. Note this pattern is viewed from the opposite side to that shown in Fig. 7 (mirror image).

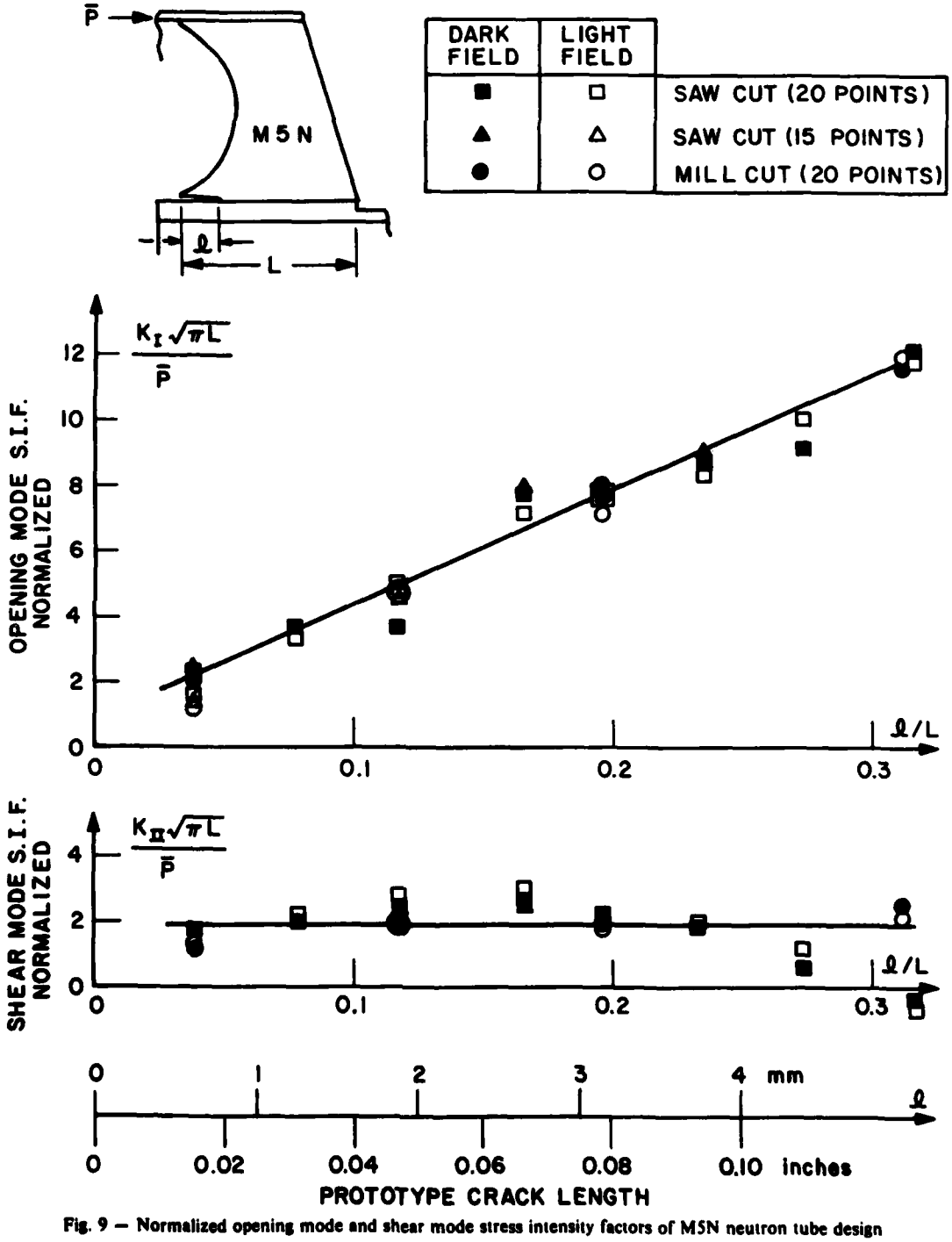

Fig. 9 — Normalized opening mode and shear mode stress intensity factors of M5N neutron tube design

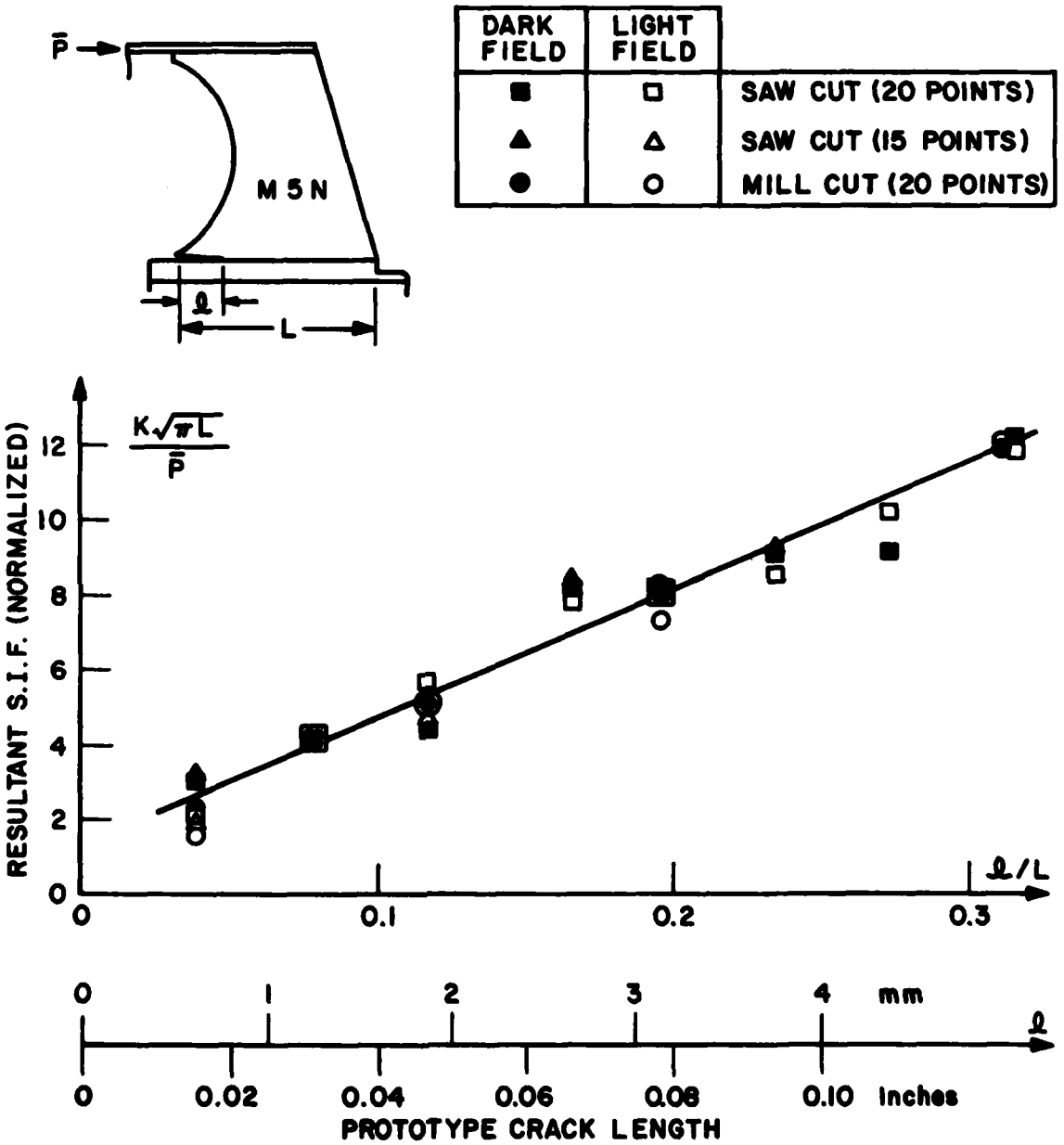

Fig. 10 — Normalized resultant stress intensity factor of M5N neutron tube design

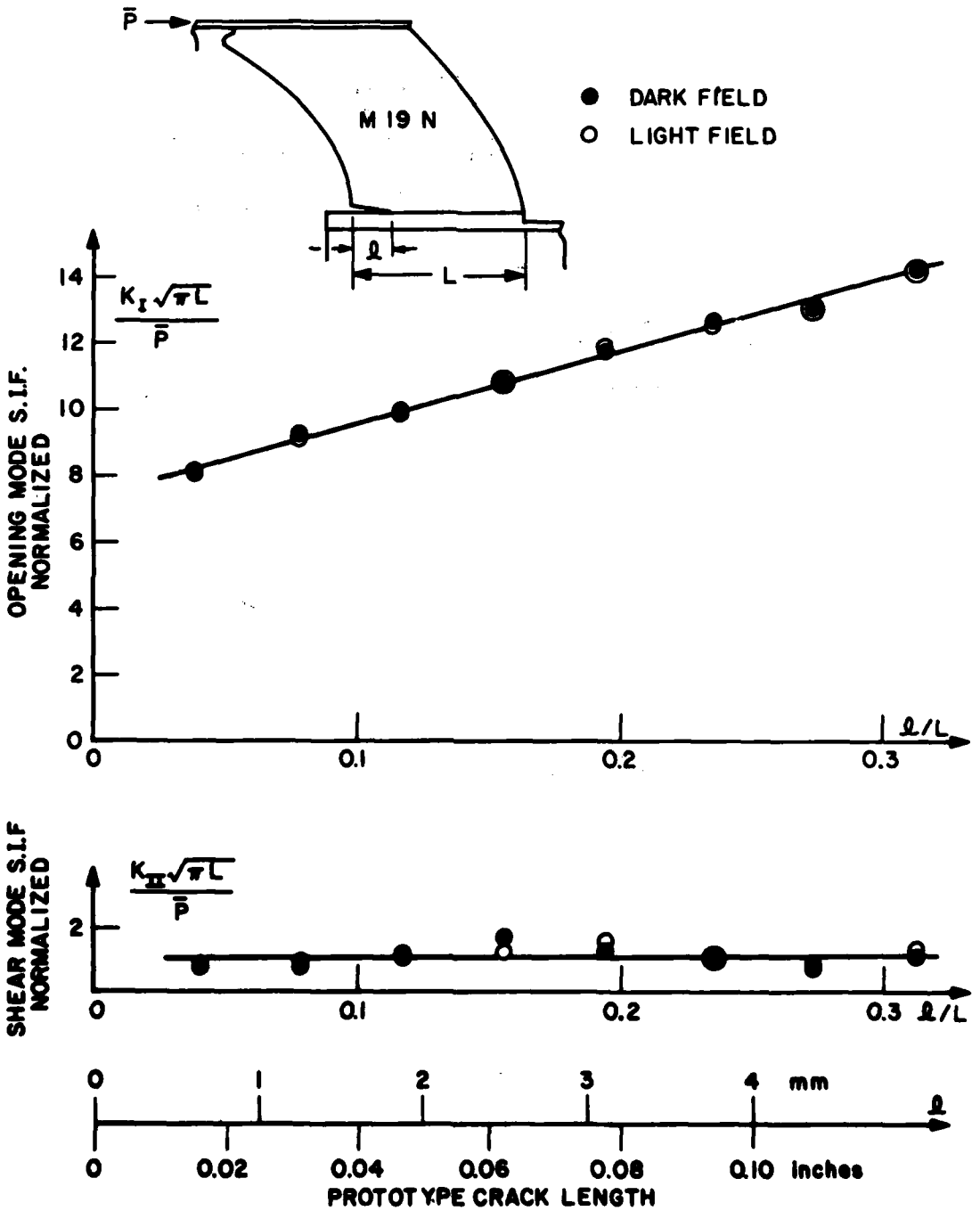

Fig. 11 — Normalized opening mode and shear mode stress intensity factors of M19N neutron tube design

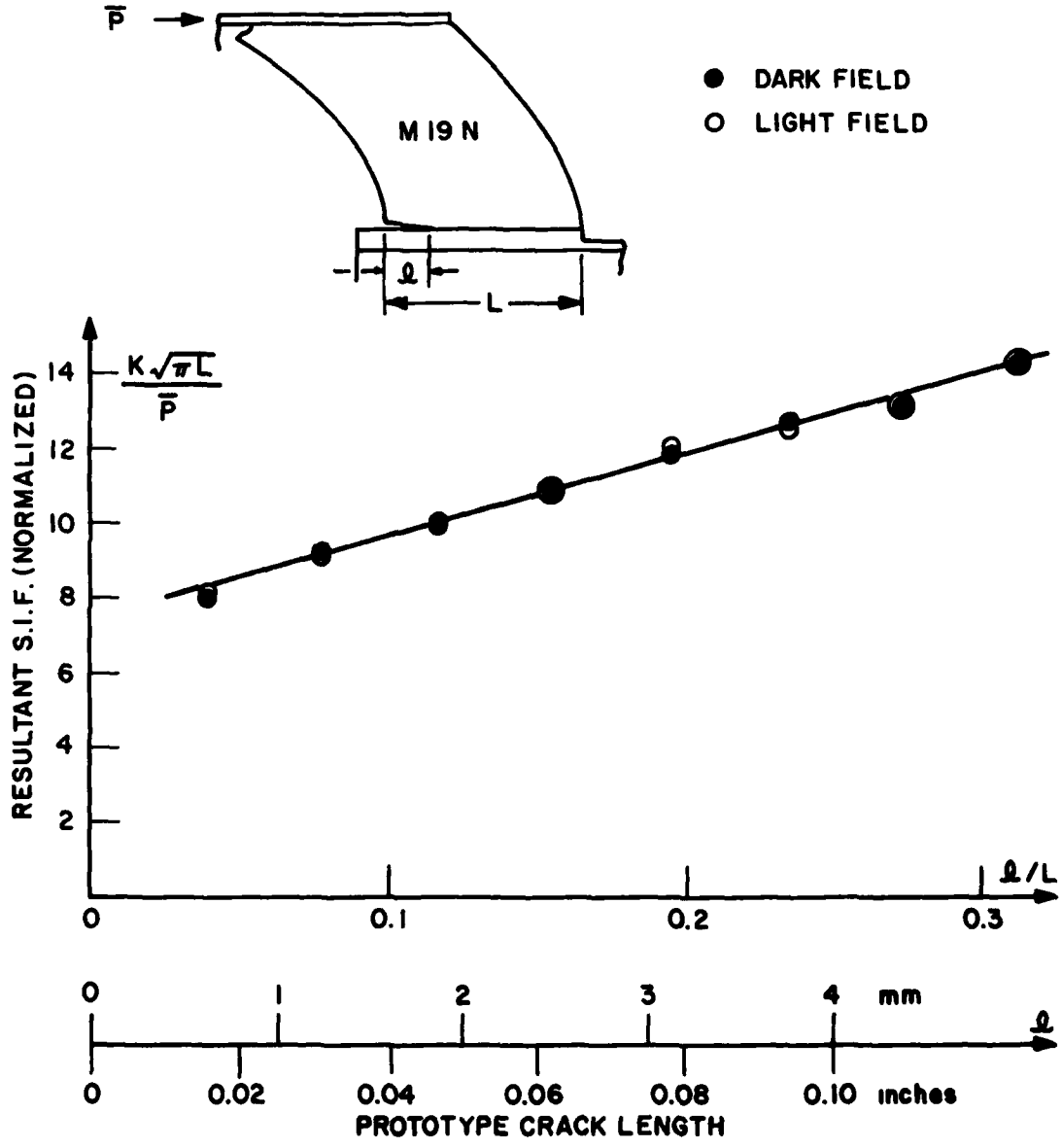

Fig. 12 — Normalized resultant stress intensity factor of M19N neutron tube design

Failure Analysis

The failure analysis reinforces the stress analysis. The M5N stress intensity factors in the critical area are lower than those in the M19N. Only after an appreciable crack length is generated in the M5N geometry, so that the crack undercuts the insulation lip, do the M5N SIF values approach the M19N values. The failure analysis also indicates that the M19N cross section is more likely to fail at the interface than the M5N cross section.

Factors Beyond the Scope of This Analysis

Certain factors outside the scope of this analysis may have a bearing on the results described and so are included here for completeness.

(1) Interface failure vs material failure

The stress analysis of the M5N cross section showed maximum stresses on the insulator halfway between the inner and outer sleeves. At first glance this would suggest a failure away from the interface. However failure on an interface between two materials can be very different in magnitude from the simple failure of either material. The following comment suggests some reasons why.

(2) Interface treatment

The type of bonding of the inner sleeve and the insulator has a great influence on interface failure. Factors in bonding that would influence failure include; local alteration of material properties or geometry, addition of a third material, or introduction of residual stresses. If these factors differ between the M5N and M19N assemblies, then they may produce results that run counter to the analyses presented here.

REFERENCES

1. Beaubien, L.A., "TOTAL: Interactive Graphics System for the Two-Dimensional Analysis of Linear Elastic Systems," Structural Mechanics Software Series, 1, N. Perrone and W. Pilkey, eds., Univ. Press of Virginia, Charlottesville (1977).

2. Sanford, R.J. and Dally, J.W., "Stress Intensity Factors in the Third-Stage Fan Disk of the TF-30 Turbine Engine," NRL Report 8202, May 15, 1978.

3. Sanford, R.J. and Dally, J.W., "A General Method for Determining Mixed-mode Stress Intensity Factors from Isochromatic Fringe Patterns" Engineering Fracture Mechanics, Vol. 11, pp. 621-633 (1979).


DAT
ILM